

Surface-Enhanced Dual-Comb Coherent Raman Spectroscopy with Nanoporous Gold Films

Ming Yan, Ling Zhang, Qiang Hao, Xuling Shen, Xiaowei Qian, Haihong Chen, Xinyi Ren, and Heping Zeng*

With two asynchronous frequency combs beating on a single detector, dual-comb spectroscopy (DCS) enables rapid, broadband, and precise molecular fingerprinting on a comb tooth-by-tooth basis and thus holds much promise in molecular sensing. Sensitivity, however, has been an Achilles' heel of this technique. Here, an approach for ultrasensitive nonlinear DCS based on plasmon-enhanced coherent Raman spectroscopy (CRS) with ultrathin (100 nm) nanoporous gold films is presented. A high-resolution ($<8\text{ cm}^{-1}$) Raman spectrum is obtained within 32.8 μs for characterizing low-density chemicals. The achieved sensitivity enhancement reaches $\approx 10^{6-8}$ relative to nonenhanced dual-comb CRS of liquid samples. The demonstrated approach may open up a new avenue for fast identification of trace amounts of chemicals.

1. Introduction

Plasmon-enhanced spectroscopy (PES) featuring ultra-high sensitivity has had a profound impact on molecular sensing and imaging.^[1–17] In principle, surface-enhanced coherent Raman spectroscopy (SECRS), a nonlinear branch of PES, is expected to offer much higher sensitivity compared to, for example, surface-enhanced Raman spectroscopy (SERS), due to multi-field enhancements.^[16,17] Its implementation, however, may have been hindered by the strict demand on plasmonic substrates in terms of resonance bandwidth. Fortunately, advanced by nanotechnology, broadband SECRS has been successfully carried out with incredible sensitivity—reaching the single-molecule level—with the aid of sharp plasmonic tips,^[12] nanoparticles,^[14,15] and nanostructured metallic substrates.^[16,17] Nevertheless, these schemes, predominately carried out with dispersive

spectrometers, share the drawbacks of limited spectral resolution and long acquisition times. These limitations also apply to SERS and present difficulties for the fast identification of unknown substances and capture of subtle spectral changes.

Dual-comb coherent anti-Stokes Raman spectroscopy (CARS) circumvents these difficulties by providing a motionless multi-photon pump-probe scheme,^[8,18–22] combining high resolution reaching the intrinsic linewidth of Raman transitions, short measurement times down to a few microseconds, high contrast against spectral background due to time and frequency filtering, and simultaneous detection, with a single detector, of a broadband spectrum. This

multiheterodyne technique has been refined by further developments respecting rapidness^[19,21] and broad bandwidth possibly covering the entire molecular fingerprint region ($400\text{--}3300\text{ cm}^{-1}$).^[18] However, detecting molecules in a sensitive manner remains challenging for this rapid dual-comb method due to its inefficient utilization of comb modes (or teeth) for broadband Raman excitation and the nonlinear nature of coherent Raman spectroscopy (CRS).

In this article, we overcome this challenge with plasmon-enhanced broadband dual-comb CRS, opening a new route to chemical sensing featured with high sensitivity and scanning-free spectral acquisition. Two frequency combs with slightly different repetition frequencies of $f_r + \Delta f$ and f_r , respectively, are focused onto molecules adsorbed on a nanoporous gold (NPG) film substrate. Two paired pulses, each from a comb, with linearly increasing time interval of τ , strike the NPG substrate and drive surface plasmons in a resonant manner, as pictured in **Figure 1a**. The localized surface plasma waves are then excited and probe vibrations of the molecules, scattering off an intensity-modulated blue-shifted anti-Stokes field which is further enhanced by the resonant plasmonic modes. Assuming that the two combs share the same field enhancement factor of g , the final anti-Stokes signal will be enhanced by g^8 , due to the four-wave mixing (FWM) process of CARS. In our proof-of-concept experiment, dual-comb sensitivity is enhanced by eight orders of magnitude. This results in the detection of monolayer molecules prepared from a 10^{-6} M solution sample with obtained Raman spectra at a resolution of $<8\text{ cm}^{-1}$ with a single-event measurement time as short as tens of microseconds.

Dr. M. Yan, Dr. X. Shen, X. Qian, X. Ren, Prof. H. Zeng
State Key Laboratory of Precision Spectroscopy
East China Normal University
Shanghai 200062, China
E-mail: hpzeng@phy.ecnu.edu.cn

Prof. L. Zhang, Dr. Q. Hao, H. Chen, Prof. H. Zeng
Shanghai Key Lab of Modern Optical System
School of Optical-Electrical and Computing Engineering
University of Shanghai for Science and Technology
Shanghai 200093, China

The ORCID identification number(s) for the author(s) of this article can be found under <https://doi.org/10.1002/lpor.201800096>

DOI: 10.1002/lpor.201800096

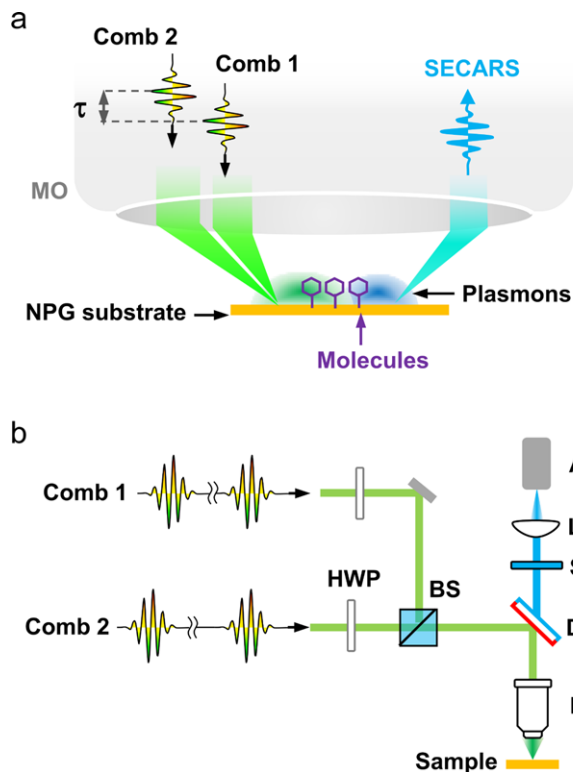


Figure 1. a) Schematic and b) experimental setup of dual-comb SECARS. APD, avalanche photodiode; BS, beamsplitter; DM, dichroic mirror; HWP, half-wave plate; MO, micro-objective lens; NPG, nanoporous gold; SPF, short-pass filter.

2. Experimental Section

The setup for dual-comb surface-enhanced coherent anti-Stokes Raman spectroscopy (SECARS) is illustrated in Figure 1b. Two frequency combs, providing sub-50 fs green pulses with similar emission spectra spanning from 518 to 545 nm (shown in Figure 2a), are employed. The polarization of each comb is adjustable through a half-wave plate. The two combs are spatially overlapped on a thin pellicle beamsplitter, and then reflected by a short-pass dichroic mirror cutting off around 510 nm, and finally focused onto a sample substrate with a microscope objective lens (RMS40X, Olympus, NA = 0.65). The coherent Raman emissions of the sample are epi-collected by the same objective lens and then spectrally filtered by the dichroic mirror and an optical short-pass filter (RPE510SP, OMEGA, cutoff wavelength at 510 nm, OD > 5) for isolating the fundamental comb beams, before being focused onto a fast, high-sensitivity avalanche photodiode (C5658, Hamamatsu) with a $f = 30$ mm lens. The detector output signal is electronically filtered by a 32 MHz low-pass filter, amplified by a low-noise electronic amplifier, and then digitized by a high-speed, 16-bit acquisition board (ATS9626, AlazarTech) at a sample rate of 180 Ms s^{-1} . The average power of each comb on the sample is about 0.15 mW.

The nanostructured substrates we use are NPG films, which have shown remarkable electromagnetic resonance properties.^[23–25] The NPG films are fabricated by chemical dealloying.^[23,24] The nanoporous structures are achieved by selec-

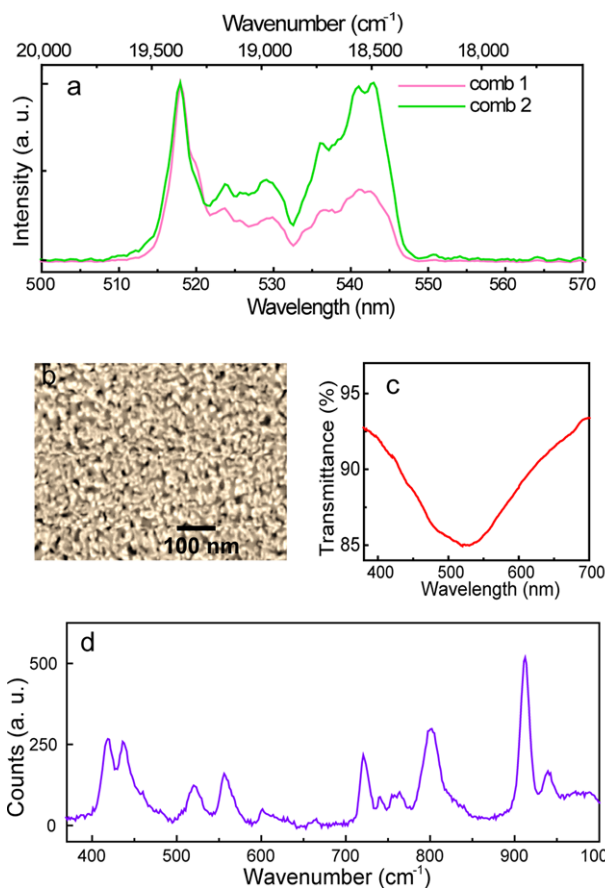


Figure 2. a) Emission spectra of the two green combs, b) the SEM micrograph, c) the transmission spectrum of an NPG film, and d) the SERS spectrum of CV molecules attached onto the NPG film. The nanopore size is estimated to be ≈ 15 nm in (b). The transmission spectrum in (c) is measured, with baseline correction, at a resolution of 0.5 nm. For (d), the sample is illuminated by a 532 nm cw laser of 0.01 mW. The Raman lines of $\nu_{33,4}(e)$ at 418 cm^{-1} , $\nu_{35}(a_1)$ at 437 cm^{-1} , $\nu_{41,2}(e)$ at 523 cm^{-1} , $\nu_{43,4}(e)$ at 560 cm^{-1} , $\nu_{50,1}(e)$ at 725 cm^{-1} , $\nu_{56,7}(e)$ at 806 cm^{-1} , $\nu_{62,3}(e)$ at 918 cm^{-1} , and $\nu_{64}(a_1)$ at 941 cm^{-1} are identified.^[26]

tively etching silver from Ag75Au25 (at.%) leaves by 65% nitric acid at room temperature for various times. The as-prepared NPG films are carefully rinsed with distilled water ($18.2 \text{ M}\Omega\text{-cm}$) to remove the remaining nitric acid. After being dealloyed for 20 s at room temperature, about $16 (\pm 5)$ % Ag remains in the films.^[23] The structure of an NPG substrate is pictured with scanning electron microscopy (SEM) and displayed in Figure 2b. The nanopore size, the equivalent diameter of nanopore channels (or gold ligaments), is characterized by a rotational fast Fourier transform analysis of the digital SEM image and found to be ≈ 15 nm.^[25] The transmission spectrum of the film, shown in Figure 2c, indicates that the ideal wavelength for excitation of the localized plasmons on the film surface is around 520 nm. Therefore, bright green lasers are desirable. The sample used in our proof-of-principle experiment is crystal violet (CV), an antibacterial chemical widely used for chemical and biomedical applications.^[26] To ensure sufficient molecule adsorption on the substrates, we immerse the NPG films in a 10^{-6} M aqueous solution for about half an hour, and then purge them with distilled water forming a monolayer of

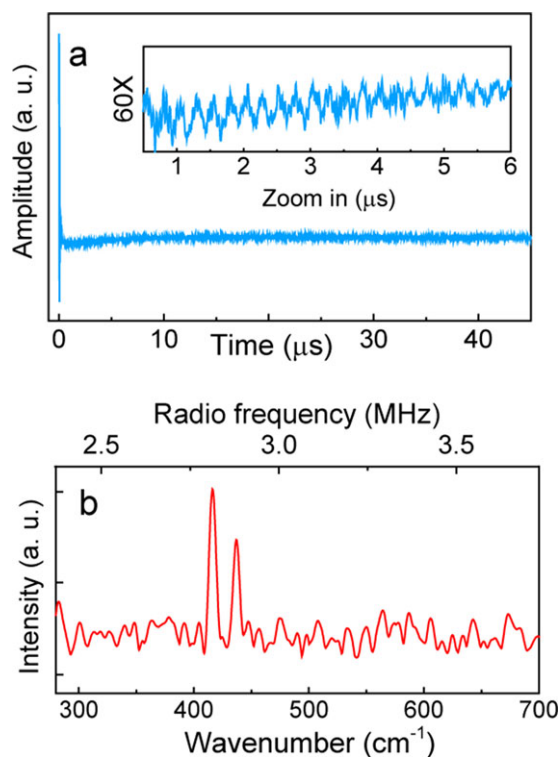


Figure 3. a) The dual-comb SECARS interferogram and b) the Fourier-transformed spectra. The zoom-in of the interferogram with $60\times$ enlargement of y -axis is shown in the inset of (a). In (b), the spectrum of single measurement is taken in $32.8\ \mu\text{s}$ with an apodized resolution of $8\ \text{cm}^{-1}$.

CV molecules, and finally dry them in air. Before the implementation of dual-comb SECARS, the specimens are tested with SERS. An enhanced Raman spectrum at a resolution of $>20\ \text{cm}^{-1}$, measured in 10 s by a micro-Raman spectrometer (RM 1000, Renishaw InVia), is displayed in Figure 2d. Several Raman lines of CV molecules are observed. The details of this measurement can be found in Supporting Information.

3. Results

Figure 3a shows a recorded dual-comb SECARS interferogram. An interferometric burst, appearing at $\tau \approx 0$, is attributed to non-resonant FWM of the two combs, which is also likely to be enhanced by the resonant plasma waves. This burst, much stronger than its interferogram tail as shown in the zoom-in of Figure 3a, is cut off when applying Fourier transform to the time-domain trace, consequently making the CARS spectrum free from non-resonant noise background. In our measurements, the repetition frequency difference (Δf) of the two combs is set to 24.5 Hz ($f_r = 108.4\ \text{MHz}$), leading to a dual-comb spectroscopy (DCS) conversion factor of $f_r/\Delta f = 4.42 \times 10^6$ which is used for rescaling the frequency axis of the Fourier transform spectrum from the radio frequency to the optical frequency (Supporting Information). The rescaled Raman spectrum of a single event is displayed in Figure 3b with an apodized resolution of $<8\ \text{cm}^{-1}$ and a measurement time of $32.8\ \mu\text{s}$. Two Raman lines of CV at 418 and $436\ \text{cm}^{-1}$, respectively, assigned to the $\nu_{33,4}(e)$ and $\nu_{35}(a_1)$

modes,^[26] are observed. The signal-to-noise ratio (SNR) for the line at $418\ \text{cm}^{-1}$ is 3.8, defined by the line peak divided by standard deviation of noise floor around $300\ \text{cm}^{-1}$. In our experiment, the SNR can be improved by spectral averaging at the cost of longer measurement times. In Figure 4a (pink curve), for instance, the 100-fold averaging takes 4 s, giving an SNR exceeding 35 for the low-wavenumber line at $418\ \text{cm}^{-1}$, where the SNRs are found evolving as square root of average times. The total average time is currently limited by our refreshing time of $1/\Delta f (= 40\ \text{ms})$ which could be further improved by up to three orders of magnitude with methods in ref. [19,21]. We also have to mention that limited dispersion management of our laser combs and the uneven enhancement of our NPG substrates across the comb emissions (518–545 nm) narrow down the interrogated Raman range. Further improvements of the substrate bandwidths are possible. For example, wrinkling the NPG surfaces^[27] or using specially designed nanosensors,^[16,17] may improve the situation with wider coverage of the more interested $800\text{--}1800\ \text{cm}^{-1}$ fingerprint region. Unfortunately, such substrates are not available in our laboratory.

To confirm the observed signals benefiting from the surface plasmon enhancement, we compare spectra for SECARS, the bare NPG substrates, and the CV solution droplets held with a thin glass plate. The three spectra, each taken in 4 s with 100-fold averaging, are shown in Figure 4a. Absence of the Raman lines in the spectra of the bare substrates (dark curve) and the droplets (dash curve) validates our dual-comb SECARS results. Meanwhile, we find that the dual-comb signal dies out after continuous illumination of about 10 s, possibly due to photodamage to the thin NPG surfaces or/and to the adsorbates by detaching them from the gold ligaments. This problem can be solved by using pulse pickers or choppers periodically blocking the unused comb pulses. The power dependence of the dual-comb SECARS is also investigated and the results are displayed in log-log scale in Figure 4b. We fit the data and find that the signal intensity of the $418\ \text{cm}^{-1}$ line relies linearly on the pump power with a slope of 1.15 ± 0.03 for the fit line (violet) and quadratically on the probe power (slope of 1.84 ± 0.03 for the fit curve in bright green). The results are consistent with our expectation as described in Supporting Information.

To evaluate the enhancement factor of our dual-comb SECARS, we conduct ordinary dual-comb CARS for a $10^{-1}\ \text{M}$ CV solution sample filled in a 0.1 mm thick cuvette. Note that detecting Raman signals of the $10^{-6}\ \text{M}$ CV solution is far beyond the capability of the nonenhanced dual-comb CARS technique. The details of the measurements, as well as the calculation, are described in Supporting Information. As a result, the comparison indicates an enhancement factor, in the best case, of 10^{6-8} for the Raman line at $418\ \text{cm}^{-1}$. Assuming that the two combs share the same enhancement effect, the field enhancement factor $g_1 (= g_2)$ for a comb is ≈ 10 , a reasonable value obtained from such NPG films.^[23-25] In fact, the enhancement effect is highly dependent on the plasmonic substrates we use. For example, Figure 5 illustrates the dual-comb SECARS spectra obtained with different NPG substrates. These substrates are fabricated with different nanopore sizes of 20 nm (NPG-2), 30 nm (NPG-3), and 35 nm (NPG-4), by increasing etching times to 60 s, 5 min, and 10 min, respectively. Inspected from the transmission spectra in Figure 5a, the spectral characteristics of the NPG

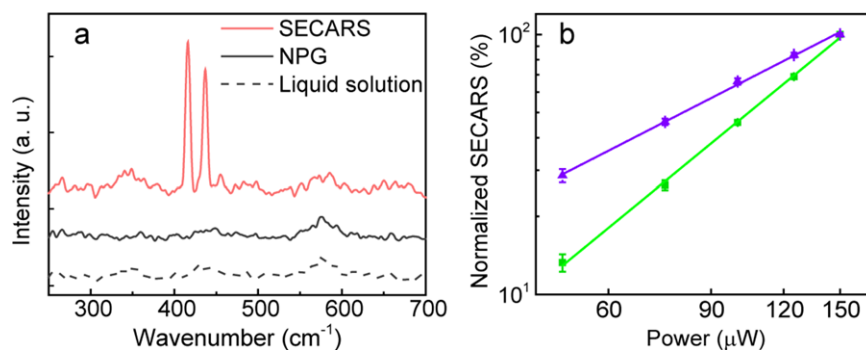


Figure 4. a) The averaged dual-comb SECARS spectra and b) the power dependences of dual-comb signal on the two combs. The spectra in (a) are averaged 100-fold with a resolution of 8 cm^{-1} . The small hills that appear around 600 cm^{-1} for the three spectra are from the background of our detection system. (b) is displayed in log–log scale and shows the dependences of the Raman signal at 418 cm^{-1} on the power of comb 1 (purple) and comb 2 (bright green). The data points are averages of 100 measurements and the error bars represent the standard deviations. The two lines with slopes of 1.15 ± 0.03 (purple) and 1.84 ± 0.03 (bright green) are the fits of the data points for comb 1 and comb 2, respectively.

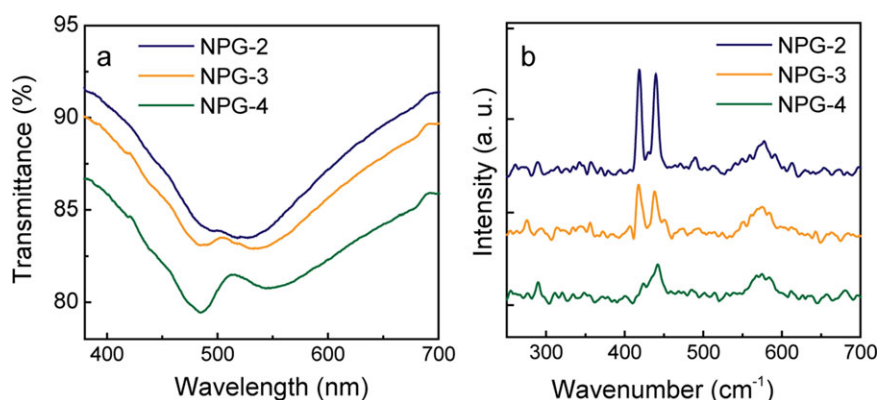


Figure 5. Comparisons of different NPG films. a) The transmission spectra of three NPG films fabricated with etching times of 60 s (NPG-2), 5 min (NPG-3), and 10 min (NPG-4), respectively. The spectra are shifted along y-axis for display. b) The dual-comb SECARS spectra of CV molecules adsorbed on the three NPG films. Each spectrum is recorded over 4 s for 100-fold averaging.

substrates change with their nanoporosity, consequently affecting their capabilities for plasmonic enhancements in terms of resonance wavelengths and enhancement strengths.^[23,24] The resulted dual-comb spectra, each taken in 4 s of 100-fold average, are shown in Figure 5b. The Raman signals are found decreasing significantly with the increased sizes of nanopores, which agrees with the results that we measured with SERS. Also, measurements conducted with different NPG films in different days indicate a certain reproducibility of our results.

4. Discussion

High-sensitivity SECARS has been previously reported by many groups. For example, first surface-enhanced stimulated Raman spectroscopy has been demonstrated for ensemble molecules attached onto “hot spots” of gold nano-antennas.^[14] In this work, an enhancement factor of 10^4 – 10^6 was achieved for broadband ($>1000\text{ cm}^{-1}$) Raman spectra averaged for 5 min at a spectral resolution of 20 cm^{-1} , although the Raman lines were presented with a large spectral background. A similar enhancement factor of $\approx 10^5$ was experimentally obtained for SECARS with nanovoid gold surfaces, resulting in Raman spectra at a resolution of

$>50\text{ cm}^{-1}$ with a single integration time of 1–100 ms.^[16] Furthermore, single-molecule sensitivity for broadband SECARS has been obtained with the help of specially designed nanostructured plasmonic substrates.^[17] The sensitivity was enhanced by $\approx 10^8$ comparing to spontaneous Raman scattering. However, limited by the spectral width ($\approx 5\text{ nm}$) of their pump laser, the spectra showed broad Raman lines of $\approx 100\text{ cm}^{-1}$. Meanwhile, high-speed, multiplex CRS has been developed for detecting chemical species in biological samples.^[28] Unfortunately, effectively combining short measurement times, high sensitivity, and specificity has not succeeded so far. Our scheme provides an enabling solution to such predicament and may lead to new spectroscopic applications, beyond static chemical sensing, such as studies of nonrepetitive chemical reactions or fast characterization of trace amounts of hazardous chemicals in water samples.

On the other hand, though ultrasensitive absorption DCS for gas-phase samples has been demonstrated with high-finesse cavities,^[29–32] hollow-core fibers,^[7] multi-pass cells,^[5,33] or by using mid- and far-infrared combs directly interrogating fundamental molecular ro-vibrational transitions,^[2,6,34–39] surface-enhanced DCS, with orders of magnitude sensitivity improvements, has not been previously introduced. Thus, our work highlights new opportunities for the field of DCS. Our

experiment here is merely carried out with NPG films and CV molecules due to limited choices in our laboratory. But, in principle, this technique is compatible with other advanced plasmonic sensors.^[14–17]

5. Conclusion

We demonstrate an ultrasensitive method for chemical sensing based on motionless SECARS with two laser combs. As an example, high-resolution Raman spectra are measured for low-density CV molecules. The measurement time for a single event can be as short as 32.8 μs supporting an apodized spectral resolution of 8 cm^{-1} . The enhancement of our CARS signals varies with the NPG substrates of different nanopore sizes. For the NPG films with 15 nm nanopores, we obtain an enhancement factor of $\approx 10^{6-8}$ for the CV 418 cm^{-1} line. The sensitivity, the spectral bandwidth, and the stability of our system are currently limited by the metal substrates we use. With further improvements of the substrates, our approach will lead to a useful tool with wide applications to physical, chemical, and environmental sciences.

Supporting Information

Supporting Information is available from the Wiley Online Library or from the author.

Acknowledgements

This work was funded in part by the National Natural Science Foundation of China (11621404, 11434005, 11561121003, 61675133, 11404211, and 11722431).

Conflict of Interest

The authors declare no conflict of interest.

Keywords

chemical sensing, coherent Raman spectroscopy, optical frequency combs, surface-enhanced spectroscopy

Received: April 8, 2018
Revised: June 25, 2018
Published online: July 31, 2018

- [1] I. Coddington, N. Newbury, W. Swann, *Optica* **2016**, *3*, 414.
- [2] F. Keilmann, C. Gohle, R. Holzwarth, *Opt. Lett.* **2004**, *29*, 1542.
- [3] T. Ideguchi, *Opt. Photonics News* **2017**, *28*, 32.
- [4] N. R. Newbury, I. Coddington, W. C. Swann, *Opt. Express* **2010**, *18*, 7929.
- [5] A. M. Zolot, F. R. Giorgetta, E. Baumann, J. W. Nicholson, W. C. Swann, I. Coddington, N. R. Newbury, *Opt. Lett.* **2012**, *37*, 638.
- [6] Y. Jin, S. M. Cristescu, F. J. M. Harren, J. Mandon, *Opt. Lett.* **2014**, *39*, 3270.
- [7] G. Millot, S. Pitois, M. Yan, T. Hovhannisyann, A. Bendahmane, T. W. Hänsch, N. Picqué, *Nat. Photonics* **2016**, *10*, 27.
- [8] T. Ideguchi, S. Holzner, B. Bernhardt, G. Guelachvili, N. Picqué, T. W. Hänsch, *Nature* **2013**, *502*, 355.
- [9] P. Stiles, J. Dieringer, N. Shah, R. Van Duyne, *Annu. Rev. Anal. Chem.* **2008**, *1*, 601.
- [10] K. Kneipp, Y. Wang, H. Kneipp, L. T. Perelman, I. Itzkan, R. R. Dasari, M. S. Feld, *Phys. Rev. Lett.* **1997**, *78*, 1667.
- [11] S. Nie, S. R. Emory, *Science* **1997**, *275*, 1102.
- [12] T. Ichimura, N. Hayazawa, M. Hashimoto, Y. Inouye, S. Kawata, *Phys. Rev. Lett.* **2004**, *92*, 220801.
- [13] E. Bailo, V. Deckert, *Chem. Soc. Rev.* **2008**, *37*, 921.
- [14] R. R. Frontiera, A. Henry, N. Gruenke, R. Van Duyne, *J. Phys. Chem. Lett.* **2011**, *2*, 1199.
- [15] S. Yampolsky, D. A. Fishman, S. Dey, E. Hulkko, M. Banik, E. O. Potma, V. A. Apkarian, *Nat. Photonics* **2014**, *8*, 650.
- [16] C. Steuwe, C. Kaminski, J. Baumberg, S. Mahajan, *Nano Lett.* **2011**, *11*, 5339.
- [17] Y. Zhang, Y.-R. Zhen, O. Neumann, J. K. Day, P. Nordlander, N. J. Halas, *Nat. Commun.* **2014**, *5*, 4424.
- [18] P. Luo, M. Yan, T. W. Hänsch, N. Picqué, presented at Light, Energy and the Environment Congress, Leipzig, Germany, November 2016, paper FW2E.2.
- [19] K. J. Mohler, B. J. Bohn, M. Yan, G. Mélen, T. W. Hänsch, N. Picqué, *Opt. Lett.* **2017**, *42*, 318.
- [20] K. Chen, T. Wu, T. Chen, H. Wei, H. Yang, T. Zhou, Y. Li, *Opt. Lett.* **2017**, *42*, 3634.
- [21] G. Mélen, M. Yan, P. Luo, T. W. Hänsch, N. Picqué, Light, Energy and the Environment Congress Leipzig, Germany, November 2016, Paper FW2E.3.
- [22] N. Coluccelli, C. R. Howle, K. McEwan, Y. Wang, T. T. Fernandez, A. Gambetta, P. Laporta, G. Galzerano, *Opt. Lett.* **2017**, *42*, 4683.
- [23] L. Zhang, L. Chen, H. Liu, Y. Hou, A. Hirata, T. Fujita, M. Chen, *J. Phys. Chem. C* **2011**, *115*, 19583.
- [24] X. Lang, P. Guan, L. Zhang, T. Fujita, M. Chen, *Appl. Phys. Lett.* **2010**, *96*, 073701.
- [25] L. Chen, L. Zhang, T. Fujita, M. Chen, *J. Phys. Chem. C* **2009**, *113*, 14195.
- [26] M. Vega Cañamares, C. Chenal, R. L. Birke, J. R. Lombardi, *J. Phys. Chem. C* **2008**, *112*, 20295.
- [27] L. Zhang, X. Lang, A. Hirata, M. Chen, *ACS Nano* **2011**, *5*, 4407.
- [28] C. H. Camp, Jr, M. T. Cicerone, *Nat. Photonics* **2015**, *9*, 295.
- [29] B. Bernhardt, A. Ozawa, P. Jacquet, M. Jacquy, Y. Kobayashi, T. Udem, R. Holzwarth, G. Guelachvili, T. W. Hänsch, N. Picqué, *Nat. Photonics* **2010**, *4*, 55.
- [30] F. Adler, M. J. Thorpe, K. C. Cossel, J. Ye, *Annu. Rev. Anal. Chem.* **2010**, *3*, 175.
- [31] R. Grilli, G. Méjean, C. Abd Alrahman, I. Ventrillard, S. Kassi, D. Romanini, *Phys. Rev. A* **2012**, *85*, 051804.
- [32] M. A. Reber, Y. Chen, T. K. Allison, *Optica* **2016**, *3*, 311.
- [33] S. Okubo, K. Iwakuni, H. Inaba, K. Hosaka, A. Onae, H. Sasada, F. Hong, *Appl. Phys. Express* **2015**, *8*, 082402.
- [34] F. Zhu, A. Bicer, R. Askar, J. Bounds, A. A. Kolomenskii, V. Kelessides, M. Amani, H. A. Schuessler, *Laser Phys. Lett.* **2015**, *12*, 095701.
- [35] Z. Zhang, T. Gardiner, D. T. Reid, *Opt. Lett.* **2013**, *38*, 3148.
- [36] G. Villares, A. Hugi, S. Blaser, J. Faist, *Nat. Commun.* **2014**, *5*, 5192.
- [37] A. Hugi, G. Villares, S. Blaser, H. Liu, J. Faist, *Nature* **2012**, *492*, 229.
- [38] G. Ycas, F. R. Giorgetta, E. Baumann, I. Coddington, D. Herman, S.A. Diddams, N. R. Newbury, arXiv:1709.07105, **2017**.
- [39] M. Yan, P. Luo, K. Iwakuni, G. Millot, T. W. Hänsch, N. Picqué, *Light Sci. Appl.* **2017**, *6*, e17076.